Inorg. Chem. **2005**, *44*, 1973–1982

Synthesis, Crystal Structures, and Nonlinear Optical (NLO) Properties of New Schiff-Base Nickel(II) Complexes. Toward a New Type of Molecular Switch?

Jean Pierre Costes, Jean François Lamère, Christine Lepetit, Pascal G. Lacroix,* and Françoise Dahan

Laboratoire de Chimie de Coordination du CNRS, 205 route de Narbonne, 31077 Toulouse, France

Keitaro Nakatani

PPSM, Ecole Normale Supérieure de Cachan, UMR 8531, 61 Avenue du Pdt Wilson, 94235 Cachan, France

Received October 11, 2004

An H_2L Schiff-base ligand that was obtained from the monocondensation of diaminomaleonitrile and 4-(diethylamino)-salicylaldehyde is reported together with four related nickel(II) complexes formulated as [Ni(L)(L′)] (L′ = $MePhCHNH_2$, $^iPrNH_2$, Py, and PPh_3). Crystal structures have been solved for H_2L, [Ni(L)($MePhCHNH_2$)], and [Ni(L)($^iPrNH_2$)]. Surprisingly, the complexation process leads to the formation of a rather unusual nickel amido (–NH–Ni^{II}) bond by deprotonation of the primary amine of H_2L. A reduction of the quadratic hyperpolarizability (β) from 38×10^{-30} to 17.5×10^{-30} cm^5 esu^{-1} is evidenced on H_2L upon metal complexation by the electric-field-induced second-harmonic (EFISH) technique. Qualitative ZINDO/SCI quantum chemical calculations indicate that, in [Ni(L)($MePhCHNH_2$)], the β orientation strongly depends on the laser wavelength. In particular, a β rotation strictly equal to 90° could be obtained with 1.022 μm incident light on passing from [Ni(L)($MePhCHNH_2$] to a hypothetical [Ni(HL)($MePhCHNH_2$]$^+$ protonated complex, thus raising the possibility for a new type of molecular switch.

Introduction

For about four decades, molecular chemistry has provided intriguing benchmark units that are used widely to test various models that describe the electronic behaviors of solids. Magnetism,[1,2] electronic conductivity,[3] and nonlinear optics[4,5] have been the most explored properties in these derivatives. Besides an academic interest, these have also been expected to possess unique capabilities, such as enhanced properties with respect to the traditional (non-molecular) materials in some cases, highly anisotropic electronic behaviors, or the possibility of leading to multifunction components in relation to the emerging concept of molecular switches.[6,7] This is especially true in nonlinear optics, for which molecular chemistry has provided molecular units with greater capabilities than those of the ferroelectric crystals that are commercially available (e.g., $LiNbO_3$ or KH_2PO_4)[8] by virtue of their large hyperpolarizabilities (β),[9] together with an ultrafast response time, high damage threshold, and inherent taylorability.[10]

Over the past few years, the possibility of achieving a switch in the quadratic nonlinear optical (NLO) response has been considered.[11] Basically, most chromophores are built

* Corresponding author. E-mail: pascal@lcc-toulouse.fr.

(1) Kahn, O. *Molecular Magnetism*; VCH: Weinheim, Germany, 1993.
(2) Miller, J. S.; Epstein, A. J. *Angew. Chem., Int. Ed. Engl.* **1994**, *33*, 385.
(3) See, for example, Special Issue on Molecular Conductors. *J. Mater. Chem.* **1995**, *5*(10).
(4) Optical Nonlinearity in Chemistry, a special issue of *Chem. Rev.* **1994**, *94* (Jan).
(5) (a) *Molecular Nonlinear Optics: Materials, Physics and Devices*; Zyss, J., Ed.; Academic Press: Boston, 1994. (b) *Nonlinear Optics of Organic Molecules and Polymers*; Nalwa, H. S., Miyata, S., Eds; CRC Press: New York, 1997.
(6) Lehn, J.-M. *Supramolecular Chemistry: Concepts and Perspectives*; VCH: Weinheim, Germany, 1995.
(7) Ward, M. D. *Chem. Soc. Rev.* **1995**, *24*, 121.
(8) Kurtz, S. K. In *Laser Handbook*; Arecchi, F. T., Schultz-Dubois, E. O. Eds.; North-Holland: Amsterdam, 1972; Vol. 1, p 923.
(9) Williams, D. J. *Angew. Chem., Int. Ed. Engl.* **1984**, *23*, 690.
(10) (a) Dalton, L. R.; Harper, A. W.; Ghosn, R.; Steier, W. H.; Ziari, M.; Fetterman, H.; Shi, H.; Mustacich, R. V.; Jen, A. K. Y.; Shea, K. J. *Chem. Mater.* **1995**, *7*, 1060. (b) Verbiest, T.; Houbrechts, S.; Kauranen, M.; Clays, K.; Persoons, A. *J. Mater. Chem.* **1997**, *7*, 2175.

10.1021/ic048578n CCC: $30.25
Published on Web 02/12/2005

Scheme 1

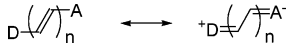

up from three components: (i) an electron-rich substituent connected through (ii) a π-electron bridge to (iii) an electron-acceptor counterpart, leading to charge delocalization by resonance, as exemplified in Scheme 1. Therefore, switching the NLO response has been achieved by changing either the donating[12] or accepting[13] strength of the substituents or by changing the conjugated capabilities[14] of the bridge. In all instances, the (on $\rightarrow$ off) switch arises invariably from a reduction of the magnitude of the quadratic hyperpolarizability, defined by the molecular polarization as follows:[9]

$$\mu_i(E) = \mu_{0i} + \alpha_{ij}E_j + \beta_{ijk}E_jE_k + ... \qquad (1)$$

In this equation, μ_0 is the permanent dipole moment, α is the polarizability, and β is the quadratic hyperpolarizability responsible for the NLO properties. Until now, the most convincing NLO switch seemed to be that reported by Coe et al,[12] who have used coordination chemistry to design ruthenium(II) complexes in which drastic β reduction is observed upon $Ru^{II} \rightarrow Ru^{III}$ oxidation.

Metal complexes exhibit charge-transfer behaviors of much greater complexity than those of the first generation of "push−pull" organic molecules that were investigated in nonlinear optics,[4,5] together with a variety of novel structures and a diversity of electronic and magnetic properties. The issue of molecular switches induced by property interplays arises naturally in metal complexes. For instance, the design of paramagnetic[15] or magnetically coupled[16] Schiff-base metal complexes with NLO responses has been envisioned. Nevertheless, the possibility for an interaction between both NLO and magnetic behaviors remains a challenging issue.[17]

In the present contribution, we will report on the synthesis, crystal structures, and NLO properties of new nickel(II) metal complexes. Their molecular structure is illustrated in Scheme 2. The effect of the metal in the environment of the ligand charge-transfer pathway will be investigated experimentally by the electric-field-induced second-harmonic (EFISH) method and computationally within the ZINDO method. In the last section, the possibility of achieving molecular switches by a β rotation instead of a β reduction will be evaluated.

Experimental Section

Materials and Equipment. 4-(Diethylamino)salicylaldehyde, diaminomaleonitrile, (*S*)-(−)-α-methylbenzylamine, isopropylamine, pyridine, and $Ni(OAc)_2 \cdot 4H_2O$ (Aldrich) were used as purchased. High-grade solvents (propane-2-ol, dichloromethane, diethyl ether, acetone, ethanol, and methanol) were used for the syntheses of ligands and complexes. Elemental analyses were carried out at the Laboratoire de Chimie de Coordination in Toulouse, France, for C, H, and N. IR spectra were recorded on a GX system 2000 Perkin-Elmer spectrophotometer. Samples were run as KBr pellets. UV−visible spectra were recorded on a Hewlett-Packard 8452A spectrophotometer. 1D ^{1}H NMR spectra were acquired at 250.13 MHz on a Bruker WM250 spectrometer. 1D ^{13}C spectra using ^{1}H broadband decoupling $\{^1H\}^{13}C$ and gated ^{1}H decoupling with selective proton irradiation were recorded with a Bruker WM250 instrument working at 62.89 MHz. Two-dimensional ^{1}H COSY experiments using standard programs and 2D pulse-field gradient HMQC ^{1}H-^{13}C correlation using a PFG-HMQC standard program were performed on a Bruker AMX400 spectrometer. Chemical shifts are given in ppm versus TMS (^{1}H and ^{13}C) using $(CD_3)_2SO$ as a solvent.

Scheme 2

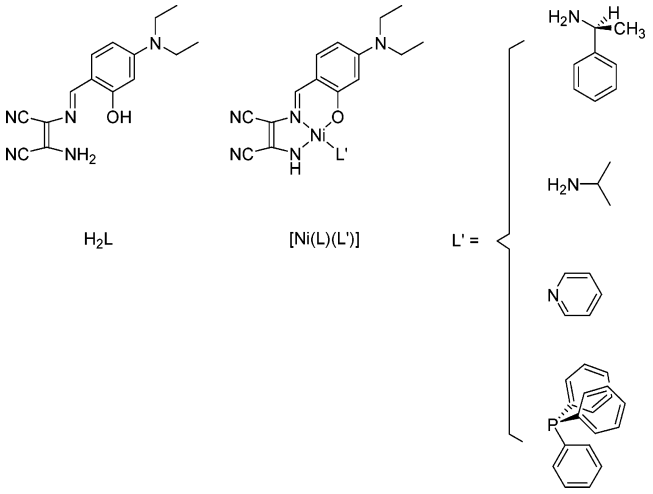

Synthesis. (2*Z*)-2-Amino-3-({(1E)-[4-(diethylamino)-2-hydroxyphenyl]methylene}amino)but-2-enedinitrile (**H_2L**): 4-(diethylamino)salicylaldehyde (1.93 g, 1×10^{-2} mol) and diaminomaleonitrile (1.08 g, 2×10^{-3} mol) were mixed in methanol (80 mL) and stirred at room temperature. The addition of 1 drop of concentrated sulfuric acid induced a color change along with immediate precipitation. The solid was filtered off 3 h later, washed with methanol and diethyl ether, and air-dried. Yield: 2.66 g (93%). Anal. Calcd for $C_{15}H_{17}N_5O$: C, 63.6; H, 6.1; N, 24.7. Found: C, 63.3; H, 5.9; N, 24.4. ^{1}H NMR (250 MHz, 20 °C, DMSO-d_6): δ 1.23 (t, J = 7 Hz, 6H, CH_3), 3.50 (q, J = 7 Hz, 4H, CH_2), 6.21 (d, J = 2 Hz, 1H, C(3)*H*), 6.41 (dd, J = 2 and 9 Hz, 1H, C(5)*H*), 7.47 (l, 2H, NH_2), 7.72 (d, J = 9 Hz, 1H, C(6)*H*), 8.46 (s, 1H, N=C*H*), 10.70 (l, 1H, O*H*). $^{13}C\{^1H\}$ NMR (62.896 MHz, 20 °C, DMSO-d_6): δ 13.4 (s, *C*H_3), 44.8 (s, *C*H_2), 97.5 (s, Ar*C*(3)H), 105.7 (s, *C*NH_2), 105.4 (s, Ar*C*(5)H), 109.9 (s, Ar*C*1), 115.2 (s, N*CC*NH_2), 116.1 (s, N*CC*N), 123.4 (s, NC*C*N),133.3 (s, Ar*C*(6)H), 152.6 (s, Ar*C*(4)NMe_2), 156.2 (s, H*C*=N), 161.5 (s, Ar*C*(2)OH). Characteristic IR absorptions (KBr): 3416, 3316, 2232, 2206,1634, 1596, 1575, 1516, 1475, 1344, 1257, 1134, 1077, 822, 783, 590 cm^{-1}.

[Ni(L)(MePhCHNH_2)]: H_2L (0.28 g, 1×10^{-3} mol), (*S*)-(−)-α-methylbenzylamine (0.12 g, 1×10^{-3} mol), and $Ni(OAc)_2 \cdot 4H_2O$ (0.25 g, 1×10^{-3} mol) were mixed in methanol (50 mL) and stirred. Heating for 15 min induced precipitation of a green powder that was filtered off, washed with methanol and diethyl ether, and air dried. Yield: 0.36 g (78%). Anal. Calcd for $C_{23}H_{26}N_6NiO$: C, 59.9; H, 5.7; N, 18.2. Found: C, 60.0; H, 5.3; N, 18.2. ^{1}H NMR (250

(11) Coe, B. J. *Chem.—Eur. J.* **1999**, *5*, 2464.
(12) See, for example, Coe, B. J.; Houbrechts, S.; Asselberghs, I.; Persoons, A. *Angew. Chem., Int. Ed.* **1999**, *38*, 366.
(13) See, for example, Hendrickx, E.; Clays, K.; Persoons, A.; Dehu, C.; Brédas, J. L. *J. Am. Chem. Soc.* **1995**, *117*, 3547.
(14) See, for example, (a) Gilat, S. L.; Kawai, S. H.; Lehn, J. M. *Chem.—Eur. J.* **1995**, *1*, 275. (b) Nakatani, K.; Delaire, J. A. *Chem. Mater.* **1997**, *9*, 2682.
(15) Di Bella, S.; Fragalà, I.; Ledoux, I.; Marks, T. J. *J. Am. Chem. Soc.* **1995**, *117*, 9481.
(16) (a) Averseng, F.; Lacroix, P. G.; Malfant, I.; Périssé, N.; Lepetit, C.; Nakatani, K. *Inorg. Chem.* **2001**, *40*, 3797. (b) Margeat, O.; Lacroix, P. G.; Costes, J. P.; Donnadieu, B.; Lepetit, C.; Nakatani, K. *Inorg. Chem.* **2004**, *43*, 4743.
(17) (a) Lacroix, P. G.; Malfant, I.; Bénard, S.; Yu, P.; Rivière, E.; Nakatani, K. *Chem. Mater.* **2001**, *13*, 441. (b) Averseng, F.; Lepetit, C.; Lacroix, P. G.; Tuchagues, J. P. *Chem. Mater.* **2000**, *12*, 2225.

MHz, 20 °C, DMSO-d_6): δ 1.20 (t, J = 7 Hz, 6H, CH_3), 1.83 (d, J = 6 Hz, 3H, CH_3), 3.45 (q, J = 7 Hz, 4H, CH_2), 3.74 and 3.86 (m, 1H + 1H, NH_2), 4.06 (m, 1H, CHNH$_2$), 5.26 (s, 1H, NH), 6.14 (d, J = 2 Hz, 1H, C(3)H), 6.36 (dd, J = 2 and 9 Hz, 1H, C(5)H), 7.39 (t, J = 7 Hz, 1H, ArCH(p)Am), 7.41 (d, J = 9 Hz, 1H, C(6)H), 7.49 (t, J = 7 Hz, 2H, ArCH(m)Am), 7.58 (d, J = 7 Hz, 2H, ArCH(o)Am), 7.71 (s, 1H, N=CH). ^{13}C{^{1}H} NMR (62.896 MHz, 20 °C, DMSO-d_6): δ 12.9 (s, CH$_3$), 24.4 (s, CH$_3$Am), 44.0 (s, CH$_2$), 51.2 (s, CHAm), 99.0 (s, ArC(3)H), 101.6 (s, CNH), 104.5 (s, ArC(5)H), 111.3 (s, ArC1), 113.2 (s, NCCNH), 116.1 (s, NCCN), 126.7 (s, ArCHAm), 127.4 (s, ArCHAm), 128.5 (s, ArCHAm), 129.9 (s, NCCN),133.6 (s, ArC(6)H), 144.2 (s, ArCAm), 147.4 (s, HC=N), 151.0 (s, ArC(4)NMe$_2$), 163.7 (s, ArC(2)O). Characteristic IR absorptions (KBr): 3325, 2222, 2167, 1611, 1583, 1557, 1504, 1403, 1369, 1353, 1267, 1246, 1217, 1141, 1063, 815, 775, 699, 637, 528 cm^{-1}.

[Ni(L)(^{i}PrNH$_2$)]: This complex was prepared in the same manner as the previous one with the use of isopropylamine. The solution was set aside for 24 h, and green crystals appeared. Yield: 0.13 g (63%). Anal. Calcd for $C_{18}H_{24}N_6NiO$: C, 54.2; H, 6.1; N, 21.1. Found: C, 53.9; H, 5.9; N, 20.9. ^{1}H NMR (250 MHz, 20 °C, DMSO-d_6): δ 1.19 (t, J = 7 Hz, 6H, CH_3), 1.48 (d, J = 6.5 Hz, 6H, CH_3), 2.98 (sept, 1H, CHNH$_2$), 3.23 and 3.25 (s, 1H + 1H, NH_2), 3.43 (q, J = 7 Hz, 4H, CH_2), 5.25 (s, 1H, NH), 6.07 (d, J = 2 Hz, 1H, C(3)H), 6.36 (dd, J = 2 and 9 Hz, 1H, C(5)H), 7.41 (d, J = 9 Hz, 1H, C(6)H), 7.74 (s, 1H, N=CH). ^{13}C{^{1}H} NMR (62.896 MHz, 20 °C, DMSO-d_6): δ 12.9 (s, CH$_3$), 24.1 (s, CH$_3$Am), 43.9 (s, CH$_2$), 43.9 (s, CHAm), 99.0 (s, ArC(3)H), 101.5 (s, CNH), 104.4 (s, ArC(5)H), 111.3 (s, ArC1), 113.1 (s, NCCNH), 115.5 (s, NCCN), 130.1 (s, NCCN),133.6 (s, ArC(6)H), 147.4 (s, HC=N), 151.0 (s, ArC(4)NMe$_2$), 163.7 (s, ArC(2)O). Characteristic IR absorptions (KBr): 3300, 3243, 2218, 2168, 1612, 1583, 1558, 1500, 1403, 1373, 1352, 1264, 1240, 1215, 1192, 1138, 1076, 820, 780, 697, 640, 526 cm^{-1}.

[Ni(L)(Py)]: This complex was prepared in the same manner as the previous one with the use of pyridine. It precipitated quickly as a powder that was filtered off, washed with methanol and diethyl ether, and air dried. Yield: 0.11 g (50%). Anal. Calcd for $C_{20}H_{20}N_6$-NiO: C, 57.3; H, 4.8; N, 20.1. Found: C, 57.0; H, 4.9; N, 19.9. ^{1}H NMR (250 MHz, 20 °C, DMSO-d_6): δ 1.18 (t, J = 7 Hz, 6H, CH_3), 3.42 (q, J = 7 Hz, 4H, CH_2), 5.96 (l, 1H, NH), 6.02 (s, 1H, C(3)H), 6.39 (d, J = 9 Hz, 1H, C(5)H), 7.49 (d, J = 9 Hz, 1H, C(6)H), 7.76 (l, 2H, CH(m)Py), 8.14 (t, J = 7 Hz, 1H, CH(p)Py), 9.13 (l, 2H, CH(o)Py), 10.03 (s, 1H, N=CH). ^{13}C{^{1}H} NMR (62.896 MHz, 20 °C, DMSO-d_6): δ 12.8 (s, CH$_3$), 43.9 (s, CH$_2$), 104.9 (s, ArC(5)H), 112.0 (s, ArC1), 125.9 (l, CH(m)Py), 133.4 (s, ArC(6)H), 138.6 (l, CH(p)Py), 148.4 (s, HC=N), 151.1 (l, CH-(o)Py), 151.9 (s, ArC(4)NMe$_2$), 164.3 (s, ArC(2)O). Characteristic IR absorptions (KBr): 3354, 2217, 2178, 1608, 1579, 1566, 1500, 1404, 1362, 1351, 1269, 1238, 1218, 1139, 1127, 1073, 820, 766, 698, 600, 526 cm^{-1}.

[Ni(L)(PPh$_3$)]: H_2L (0.28 g, 1 × 10^{-3} mol), PPh$_3$ (0.30 g, 1 × 10^{-3} mol), and Ni(OAc)$_2$·4H$_2$O (0.25 g, 1 × 10^{-3} mol) were mixed in methanol (50 mL) and stirred. Heating for 15 min induced precipitation of a black powder that was filtered off, washed with methanol and diethyl ether, and air dried. Yield: 0.58 g (95%). Anal. Calcd for $C_{33}H_{30}N_5NiOP$: C, 65.8; H, 5.0; N, 11.6. Found: C, 65.9; H, 5.0; N, 11.5. ^{1}H NMR (250 MHz, 20 °C, DMSO-d_6): δ 1.15 (t, J = 7 Hz, 6H, CH_3), 3.36 (q, J = 7 Hz, 4H, CH_2), 5.63 (l, 1H, NH), 6.38 (d, J = 9 Hz, 1H, C(5)H), 7.52 (d, J = 9 Hz, 1H, C(6)H), 7.65 (s, 15H, CH PPh$_3$), 7.73 (s, 1H, N=CH). ^{13}C{^{1}H} NMR (62.896 MHz, 20 °C, DMSO-d_6): 12.7 (s, CH$_3$), 44.1 (s, CH$_2$), 105.0 (s, ArC(5)H), 128.9 (s, ArCHPhos), 130.8 (s, ArCH-Phos), 134.2 (s, ArCHPhos), 148.0 (s, HC=N), 151.9 (s, ArC(4)-NEt$_2$). Characteristic IR absorptions (KBr): 3366, 2218, 2178, 1609, 1583, 1565, 1514, 1496, 1435, 1351, 1269, 1242, 1213, 1140, 1097, 826, 752, 695, 528 cm^{-1}.

Structure Analysis and Refinement. Crystal data for H_2L and [Ni(L)(MePhCHNH$_2$)] were collected on an Enraf-Nonius CAD4 diffractometer using graphite-monochromated Mo Kα radiation (λ = 0.71073 Å). Final unit cell parameters were obtained by means of least-squares refinement of a set of 25 reflections in both crystal structures. No significant standard intensity variations (±0.5%) were observed. Semiempirical absorption corrections from psi scans were applied to the nickel complex.[18] The data for [Ni(L)(^{i}PrNH$_2$)] were collected on a Stoe imaging plate diffraction system (IPDS) equipped with an Oxford Cryosystems cooler device using a graphite-monochromated Mo Kα radiation (λ = 0.71073 Å). Absorption corrections were applied (T_{min} = 0.5805, T_{max} = 0.7691).[19]

The three crystal structures were solved by means of direct methods using SHELXS-97[20] and refined by least-squares procedures on F_o^2 using SHELXL-97.[21] In H_2L, the N(3), C(8), C(9), C(10), and C(11) atoms of the diethylamino substituent were found to be disordered. Their occupancy factors were first refined and then kept fixed in the ratio 55/45. H atoms were introduced into calculations with the rigid model, with Uiso equal to 1.1 times that of the atom of attachment. Scattering factors were taken from the International Tables for Crystallography.[22] The absolute configuration was determined for [Ni(L)(MePhCHNH$_2$)] with the Flack parameter[23] using 2081 Friedel pairs. Crystallographic data are summarized in Table 1.

Theoretical Methods. Geometries were fully optimized by DFT, at the B3PW91/6-31G** level,[24] using Gaussian 98.[25] The starting geometries were those of the present X-ray structures for H_2L and [Ni(L)(MePhCHNH$_2$)]. [Ni(L)(MePhCHNH$_2$)] was used as a model for the starting geometry of [Ni(HL)(MePhCHNH$_2$)]$^+$. Vibrational analysis was performed at the same level to check the attainment of a minimum on the potential energy surface and to compute zero-point vibrational energies. The calculated structures are in good agreement with the crystallographic data that is available (vide infra). The calculated structures of H_2L, [Ni(L)(MePhCHNH$_2$)], and [NiH(L)(MePhCHNH$_2$)]$^+$ are given in the Supporting Information.

(18) North, A. C. T.; Phillips, D. C.; Mathews, F. S. *Acta Crystallogr., Sect. A* **1968**, *24*, 351.

(19) Stoe, X. *SHAPE: Crystal Optimisation for Numerical Absorption Correction*, revision 1.01; Stoe & Cie: Darmstadt, Germany, 1996.

(20) Sheldrick, G. M. *SHELXS-97: Program for Crystal Structure Solution*; University Of Göttingen: Göttingen, Germany, 1990.

(21) Sheldrick, G. M. *SHELXL-97: Program for the Refinment of Crystal Structures from Diffraction Data*; University Of Göttingen: Göttingen, Germany, 1997.

(22) *International Tables for Crystallography*; Kluwer Academic Publishers: Dordrecht, The Netherlands, 1992; Vol. C, Tables 4.2.6.8 and 6.1.1.4.

(23) Flack, H. D. *Acta Crystallogr., Sect. A* **1983**, *39*, 876.

(24) (a) Becke, A. D. *J. Chem. Phys.* **1993**, *98*, 564. (b) Perdew, J. P.; Wang, Y. *Phys. Rev. B* **1992**, *45*, 13244.

(25) Frisch, M. J.; Trucks, G. W.; Schlegel, H. B.; Scuseria, G. E.; Robb, M. A.; Cheeseman, J. R.; Zakrzewski, V. G.; Montgomery, J. A., Jr.; Stratmann, R. E.; Burant, J. C.; Dapprich, S.; Millam, J. M.; Daniels, A. D.; Kudin, K. N.; Strain, M. C.; Farkas, O.; Tomasi, J.; Barone, V.; Cossi, M.; Cammi, R.; Mennucci, B.; Pomelli, C.; Adamo, C.; Clifford, S.; Ochterski, J.; Petersson, G. A.; Ayala, P. Y.; Cui, Q.; Morokuma, K.; Malick, D. K.; Rabuck, A. D.; Raghavachari, K.; Foresman, J. B.; Cioslowski, J.; Ortiz, J. V.; Stefanov, B. B.; Liu, G.; Liashenko, A.; Piskorz, P.; Komaromi, I.; Gomperts, R.; Martin, R. L.; Fox, D. J.; Keith, T.; Al-Laham, M. A.; Peng, C. Y.; Nanayakkara, A.; Gonzalez, C.; Challacombe, M.; Gill, P. M. W.; Johnson, B. G.; Chen, W.; Wong, M. W.; Andres, J. L.; Head-Gordon, M.; Replogle, E. S.; Pople, J. A. *Gaussian 98*, revision A.7; Gaussian, Inc.: Pittsburgh, PA, 1998.

Table 1. Crystal Data for H_2L, [Ni(L)(MePhCHNH$_2$)], and [Ni(L)(^{i}PrNH$_2$)]

	H_2L	[Ni(L)(MePhCHNH$_2$)]	[Ni(L)(^{i}PrNH$_2$)]
cryst data			
chemical formula	$C_{15}H_{17}N_5O$	$C_{23}H_{26}N_6NiO$	$C_{18}H_{24}N_6NiO$
mol wt	283.34	461.21	399.14
cryst size (mm)	0.5 × 0.2 × 0.1	0.5 × 0.15 × 0.1	0.5 × 0.5 × 0.4
cryst syst	monoclinic	orthorhombic	monoclinic
space group	$P2_1/n$	$P2_12_12_1$	$P2_1/n$
a (Å)	21.080(2)	13.9124(13)	10.5988(11)
b (Å)	7.2369(9)	25.076(2)	14.1297(12)
c (Å)	9.9220(11)	6.4440(9)	13.0200(14)
β (deg)	91.695(9)		100.790(13)
V (Å^3)	1513.0(3)	2248.1(4)	1915.4(3)
ρ_{calcd} (Mg/m^3)	1.244	1.363	1.384
μ (Mo Kα) (mm^{-1})	0.083	0.890	1.032
T (K)	293	293	180
data collection			
radiation (Mo Kα) (Å)	0.71073	0.71073	0.71073
scan mode	$\omega - 2\theta$	$\omega - 2\theta$	ϕ
scan range			$0 < \phi < 250.5°$
2θ range (deg)	2.95−54	2.95−54	2.15−26.04
no. of reflns			
measured	3482	5692	18357
unique	3303	4898	3710
observed [$I > 2\sigma(I)$]	1139	3669	3375
refinement			
refinement on	F_o[b]	F_o[b]	F_o[b]
no. of variables	235	283	235
H-atom treatment	calcd	calcd	calcd
R [$I > 2\sigma(I)$][a]	0.0320	0.0276	0.0276
wR2[b]	0.0701	0.0541	0.0539
$\Delta\rho_{max}$ (e Å^{-3})	0.109	0.211	0.259
$\Delta\rho_{min}$ (e Å^{-3})	−0.116	−0.156	−0.324
Flack parameter		−0.012(11)	

[a] $R = (\sum|F_o| - |F_c|)/(\sum|F_o|)$. [b] wR2 = $\{[\sum(w(Fo^2 - Fc^2)^2)]/[\sum(w(Fo^2)^2)]\}^{1/2}$.

Proton affinities (PA) were calculated as the negative of the enthalpy changes at 0 K for the addition of a proton to the molecule M ($M_{(g)} + H_{(g)}^+ \rightarrow MH_{(g)}^+$). The enthalpy changes were obtained according to the standard definition of proton affinity[26]

$$(PA)_{0\,K} = E(M) + ZPE(M) - E(MH^+) - ZPE(MH^+) \quad (2)$$

where E stands for the electronic energy and ZPE stands for the zero-point vibrational energy.

The all-valence INDO (intermediate neglect of differential overlap) formalism,[27] in connection with the sum over state (SOS) formalism, was employed for the calculation of the electronic spectra and the molecular hyperpolarizabilities.[28] In the present approach, the monoexcited configuration interaction (CIS) approximation was employed to describe the excited states. The lowest 100 energy transitions were chosen to undergo CI mixing. All of the calculations were performed using the INDO/1 Hamiltonian incorporated into the commercially available software package ZINDO.[29]

NLO Measurements. The molecular hyperpolarizabilities were investigated by the electric-field-induced second-harmonic (EFISH) technique for H_2L and [Ni(L)(MePhCHNH$_2$)]. The principle of the EFISH technique is reported elsewhere.[30] The data were recorded using a nanosecond Nd:YAG pulsed (10-Hz) laser operating at $\lambda = 1.064$ μm. The outcoming Stokes-shifted radiation at $\lambda = 1.907$ μm that was generated by Raman effect in a hydrogen cell (1 m long, 50 atm) was used as the fundamental beam for second-harmonic generation (SHG). The compounds were dissolved in dioxane at various concentrations (0 to 2×10^{-2} mol L^{-1}). The centrosymmetry of the solution was broken by the dipolar orientation of the chromophores with a high-voltage pulse (5 kV) synchronized with the laser pulse. The SHG signal was selected through a suitable interference filter, detected by a photomultiplier, and recorded on an ultrafast Tektronic TDS 620 B oscilloscope. With the NLO response being induced by dipolar orientation of the chromophores, the EFISH signal is therefore a function of both the dipole moment (μ) and β_{vec}, the vector component of β along the dipole moment direction. However, the ZINDO calculation reveals that μ and β_{vec} are roughly parallel at 1.907 μm with angle values equal to 8 and 10° for H_2L and [Ni(L)(MePhCHNH$_2$)], respectively. Therefore, β_{vec} and β are assumed to be equivalent for the present EFISH measurement. The dipole moments were measured independently by a classic method based on the Guggenheim theory.[31] Further details of the experimental methodology and data analysis are reported elsewhere.[32]

In addition, the measurement of second-harmonic generation (SHG) intensity on [Ni(L)(MePhCHNH$_2$)] was carried out by the Kurtz−Perry powder technique[33] using the same laser equipment.

(26) Youjung, S.; Yangsoo, K.; Yongho, K. *Chem. Phys. Lett.* **2001**, *340*, 186.

(27) (a) Zerner, M.; Loew, G.; Kirchner, R.; Mueller-Westerhoff, U. *J. Am. Chem. Soc.* **1980**, *102*, 589. (b) Anderson, W. P.; Edwards, D.; Zerner, M. C. *Inorg. Chem.* **1986**, *25*, 2728.

(28) Ward, J. F. *Rev. Mod. Phys.* **1965**, *37*, 1.

(29) *ZINDO*, release 96.0; Molecular Simulations Inc.: Cambridge, U.K., 1996

(30) (a) Oudar, J. L. *J. Chem. Phys.* **1977**, *67*, 446. (b) Levine, B. F.; Betha, C. G. *J. Chem. Phys.* **1975**, *63*, 2666. Levine, B. F.; Betha, C. G. *J. Chem. Phys.* **1976**, *65*, 2429.

(31) Guggenheim, E. A. *Trans. Faraday Soc.* **1949**, *45*, 714.

(32) Malthey, I.; Delaire, J. A. Nakatani, K.; Wang, P.; Shi, X.; Wu, S. *Adv. Mater. Opt. Electron.* **1996**, *6*, 233.

Samples were uncalibrated powders obtained by grinding and were put between two glass plates.

Results and Discussion

Synthesis and Characterization. H_2L is obtained readily by simple mixing of 4-(diethylamino)salicylaldehyde and diaminomaleonitrile in alcohol in a 1/1 ratio. Sulfuric acid has been used previously as a catalyst in the synthesis of Schiff bases that are built up from the present weakly reacting diaminomaleonitrile.[34,35] ^{1}H and ^{13}C NMR and elemental analysis confirm the composition of the resulting monoimine. IR spectroscopy provides additional evidence of the monoimine nature of the compound with a CN stretching mode split into two components at 2232 and 2206 cm^{-1}, in contrast to the single band that is observed at 2210 cm^{-1} in the symmetric and related diimine ligand that was reported previously.[34]

The synthesis of the nickel(II) complexes requires the use of a stoichiometric amount (or a slight excess of a coordinating amine or phosphine). For instance, no reaction is observed by heating H_2L and $Ni(OAc)_2{\cdot}4H_2O$ in the presence of a 10-fold excess of NEt_3, whereas H_2L, $NiCl_2{\cdot}6H_2O$, and a primary amine in stoichiometric amounts (1/1) lead to the desired complex with the deprotonation of H_2L. This last chemical feature is evidenced by IR spectroscopy by the presence of a narrow peak in the 3350−3300-cm^{-1} domain that is attributed to the NH stretching vibration of the R−NH^- function. This is identified clearly in [Ni(L)(py)] in which no other NH band can interfere. Additional evidence is provided by the ^{1}H NMR spectra with a signal located around 6 ppm in each complex (intensity = 1H). The final assignment for the ^{13}C NMR signal required the use of 2D NMR, especially for the diaminomaleonitrile fragments. It may be interesting to point out that in the case of [Ni(L)(py)] no diaminomaleonitrile signal is observed, probably because of the rotation of the pyridine ligand, which results in a broadening of the NMR signals. Similarly, the ^{1}H and ^{13}C pyridine signals are broad, except for the CH in the para position with respect to the nitrogen atom, for which a sharper signal is observed.

Deprotonation of the primary amine function of the tridentate ligand under such mild experimental conditions is very surprising and has not been observed previously in the complexation of other tridentate ligands that possess such an amine function.[36] This behavior emphasizes the role of the nitrile substituents. It has been shown, from several trials and changes in the experimental conditions, that these two deprotonations of the H_2L ligand are needed for its complexation.

Structural Studies. The X-ray molecular structure of H_2L is presented in Figure 1. The molecule crystallizes in the $P2_1/n$ space group, with one H_2L entity present in the asymmetric unit. Except for the diethylamino substituent, the molecular structure is planar with its largest deviation of 0.086(1) Å observed at N(5). The disordered nitrogen of the diethylamino group lies +0.159(7) and −0.472(9) Å from this mean plan for N(3) and N(3′), respectively. Because of the quasi-planar overall geometry, a charge transfer upon electronic transition is expected between the diethylamino substituent and the dicyano moieties, thus providing a potential NLO response, as discussed in the next section.

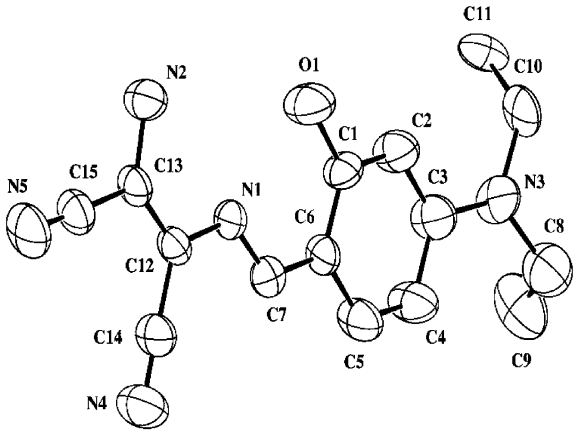

Figure 1. Asymmetric unit and atom labeling system for H_2L with ellipsoids drawn at the 50% probability level. H atoms are omitted for clarity.

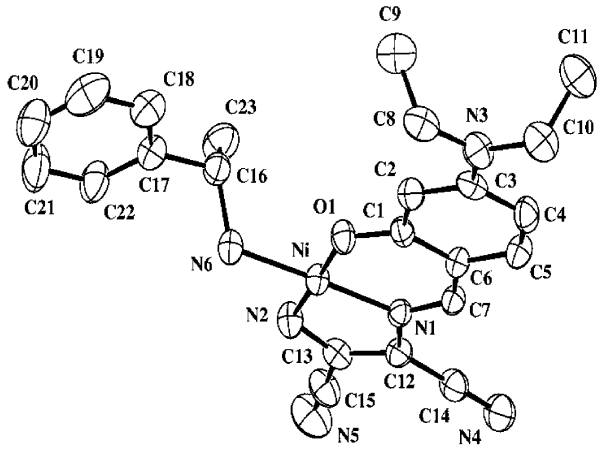

Figure 2. Asymmetric unit and atom labeling system for [Ni(L)(MePhCHNH$_2$)] with ellipsoids drawn at the 50% probability level. H atoms are omitted for clarity.

[Ni(L)(MePhCHNH$_2$)] crystallizes in the noncentrosymmetric $P2_12_12_1$ space group with one molecular entity present in the asymmetric unit. The molecular structure is shown in Figure 2. Except for the two ethyl groups, the Ni(L)N(6) fragment is planar with its largest deviation of 0.149(2) Å observed at N(4). The nickel(II) first coordination sphere is described in Table 2. The averaged metal−ligand bond lengths of 1.866(2) Å are in the same range of magnitude as that of Ni(salen) (1.850(2) Å).[37] The metal atom lies in a nearly square-planar coordination environment and is located 0.0015(3) Å from the O(1), N(1), N(2), N(6) mean plane.

[Ni(L)(^{i}PrNH$_2$)] crystallizes in the monoclinic $P2_1/n$ space group with one molecule present in the asymmetric unit. The

(33) (a) Kurtz, S. K.; Perry, T. T. *J. Appl. Phys.* **1968**, *39*, 3798. (b) Dougherty, J. P.; Kurtz, S. K. *J. Appl. Crystallogr.* **1976**, *9*, 145.
(34) Lacroix, P. G.; Di Bella, S.; Ledoux, I. *Chem. Mater.* **1996**, *8*, 541.
(35) Wöhrle, D.; Buttner, P. *Polym. Bull. (Berlin)* **1985**, *13*, 57.
(36) (a) Costes, J. P.; Dahan, F.; Dominguez-Vera, J. M.; Laurent, J. P.; Ruiz, J.; Sotiropoulos, J. *Inorg. Chem.* **1994**, *33*, 3908. (b) Costes, J. P.; Dahan, F.; Laurent, J. P. *Inorg. Chem.* **1991**, *30*, 1887.
(37) Manfredotti, A. G.; Guastini, C. *Acta Crystallogr.* **1983**, *C39*, 863.

Table 2. Selected Bond Lengths (Å) and Angles (deg) in [Ni(L)(MePhCHNH$_2$)] and [Ni(L)(^{i}PrNH$_2$)] with esd's in Parentheses

	[Ni(L)(MePhCHNH$_2$)]		[Ni(L)(^{i}PrNH$_2$)]
	X-ray	DFT	X-ray
Ni−O(1)	1.8295(15)	1.810	1.8290(10)
Ni−N(1)	1.8647(17)	1.849	1.8664(11)
Ni−N(2)	1.835(2)	1.828	1.8455(12)
Ni−N(6)	1.9349(18)	1.922	1.9259(12)
O(1)−Ni−N(1)	95.88(7)	96.1	95.73(5)
N(1)−Ni−N(2)	85.31(8)	85.5	85.46(5)
N(2)−Ni−N(6)	92.84(8)	94.2	93.06(5)
N(6)−Ni−O(1)	85.98(7)	84.1	85.97(5)
O(1)−Ni−N(2)	178.56(8)	178.3	176.57(5)
N(1)−Ni−N(6)	177.93(8)	179.7	175.83(5)

molecular structure is shown in Figure 3. The solid-state geometry of the two ethyl groups is significantly different than what was observed in [Ni(L)(MePhCHNH$_2$)]. The nickel(II) first coordination sphere is described in Table 2. As observed in [Ni(L)(MePhCHNH$_2$)], the average metal−ligand bond length is equal to 1.866 Å. The metal atom lies in a nearly perfect square-planar environment and is located 0.0041(1) Å from the O(1), N(1), N(2), N(6) mean plane. In contrast to the situation that was observed in [Ni(L)-(MePhCHNH$_2$)], the Ni(L)N(6) fragment appears to be slightly bent in the present case with its largest deviation from a mean plane being 0.323(2) observed at N(5). However, this situation may likely result from crystal packing because both [Ni(L)(MePhCHNH$_2$)] and [Ni(L)(^{i}PrNH$_2$)] exhibit very similar spectroscopic behaviors (vide infra).

In both nickel complexes, the complexation of H$_2$L induces deprotonation of the phenol function along with deprotonation of the amine function, so the ligand behaves as a dianionic four-electron donor. The resulting Ni−N amido bonds (1.835(2) and 1.845(1) Å for [Ni(L)(MePhCHNH$_2$)] and [Ni(L)(^{i}PrNH$_2$)], respectively) are shorter than the Ni−N imine bonds (1.865(2) and 1.866(1) Å) and shorter than the Ni−N amine bonds (1.935(2) and 1.926(1) Å) resulting from coordination of the primary amine ligand in the fourth position of the equatorial plane containing the nickel ion.

Gas-phase calculated geometries are in qualitative agreement with the crystal data. In particular, the molecules exhibit planar salicyleneaminato ethylene (L^{2-}) structures, which suggests the possibility of long-range electron delocalization and hence a sizable NLO response. The H$_2$L calculated geometry is very close to that obtained by X-ray. The largest difference is observed at the C(12)−C(13) bond length, with the calculated 1.380 Å value being longer than the experimental value (1.348(2) Å). Similarly, the agreement is satisfactory for [Ni(L)(MePhCHNH$_2$]. In particular, the coordination spheres of the nickel atom are compared in Table 2 and are found to be very similar, with a slight tendency for bond length shortening (<0.02 Å) in the gas-phase structure.

Optical Spectroscopy. The experimental spectra of H$_2$L and [Ni(L)(MePhCHNH$_2$)] that were recorded in acetone are compared in Figure 4. In H$_2$L, the spectrum is dominated by an intense transition located at 438 nm (ϵ = 45 800 mol^{-1} L cm^{-1}); a shoulder is present around 420 nm. The complex exhibits red-shifted but less intense transitions located at 486

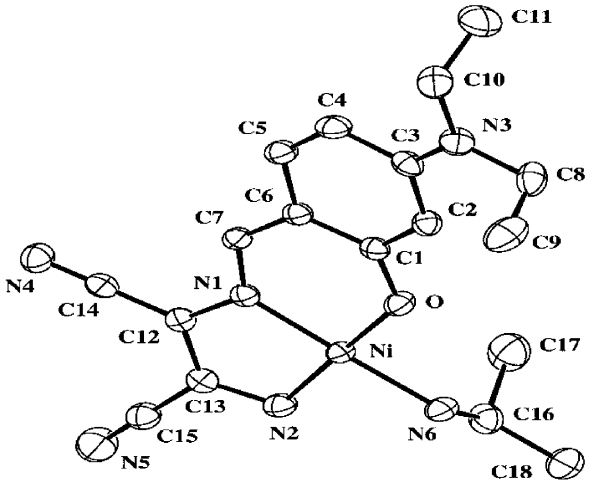

Figure 3. Asymmetric unit and atom labeling system for [Ni(L)(^{i}PrNH$_2$)] with ellipsoids drawn at the 50% probability level. H atoms are omitted for clarity.

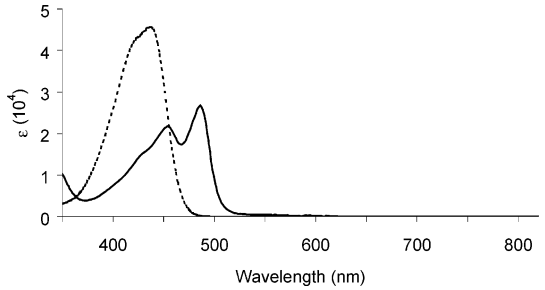

Figure 4. Electronic spectra of [Ni(L)(MePhCHNH$_2$)] in acetone compared to that of H$_2$L (dotted line).

nm (ϵ = 27 000 mol^{-1} L cm^{-1}) and 456 nm (ϵ = 21 800 mol^{-1} L cm^{-1}). Experimental spectra and ZINDO-calculated data are gathered in Table 3. There is a significant difference in λ_{max} between calculation and experiment, but the tendency for an overestimation of the energy values by means of the ZINDO approach has been observed previously in related push−pull nickel(II) Schiff-base complexes.[34,38] However, the red shift and reduced intensity obtained on passing from H$_2$L to [Ni(L)(MePhCHNH$_2$)] are observed at both experimental and theoretical levels. Similarly, the calculated relative intensities of the bands (oscillator strength *f*) are found to be comparable to the experimental extinction coefficient (ϵ) for both the ligand and the metal complex. On the basis of these observations, it will be assumed that the electronic properties that are estimated by ZINDO can be used for the analysis of the NLO response of both H$_2$L and [Ni(L)(MePhCHNH$_2$)].

All other nickel(II) complexes exhibit similar spectra with an absorption maximum located at 486 nm and an additional but less intense band at 454−456 nm (Table 3). This observation agrees fully with an NLO response dominated by the push−pull salicyleneaminato ethylene moieties, as anticipated from our previous investigations.[34,38] Because of

(38) Averseng, F.; Lacroix, P. G.; Malfant, I.; Lenoble, G.; Cassoux, P.; Nakatani, K.; Maltey-Fanton, I.; Delaire, J. A.; Aukauloo, A. *Chem. Mater.* **1999**, *11*, 995.

Table 3. Experimental and ZINDO-Computed Optical Data for H_2L and Its Related Nickel(II) Complexes

	λ_{max} (nm)		composition of CI expansion[a]
	exptl ($\epsilon \times 10^{-5}$)	calcd (f)	
H_2L	438 (0.46)	362 (1.29)	$0.965\chi_{54\rightarrow55}$
	415−425 (sh)	279 (0.23)	$0.905\chi_{54\rightarrow6}$
[Ni(L)(MePhCHNH$_2$)]	486 (0.270)	418 (0.78)	$0.966\chi_{82\rightarrow83}$
	456 (0.218)	302 (0.26)	$-0.795\chi_{82\rightarrow84}$
		296 (0.40)	$0.646\chi_{82\rightarrow83} - 0.484\chi_{82\rightarrow84}$
[Ni(HL)(MePhCHNH$_2$)]$^+$		392 (1.28)	$0.923\chi_{82\rightarrow83}$
		346 (0.13)	$0.557\chi_{80\rightarrow83} - 0.651\chi_{81\rightarrow83}$
[Ni(L)(^{i}PrNH$_2$)]	486 (0.333)		
	454 (0.255)		
[Ni(L)(Py)]	486 (0.344)		
	456 (0.267)		
[Ni(L)(PPh$_3$)]	486 (0.328)		
	454 (0.266)		

[a] Orbital 54 is the HOMO and orbital 55 the LUMO for H_2L. 82 is the HOMO and 83 is the LUMO for [Ni(L)(MePhCHNH$_2$)] and [Ni(HL)(MePhCHNH$_2$)]$^+$.

Table 4. Experimental (EFISH) and Calculated (ZINDO) Data (μ in D, β in 10^{-30} cm^5 esu^{-1}) at 1.907 μm for H_2L, [Ni(L)(MePhCHNH$_2$)], and [Ni(HL)(MePhCHNH$_2$)]$^+$

	exptl		calcd		
	μ	β	μ	β	(β_{2L}+ β_{3L})
H_2L	8.6	38	12	16.4	(23.0 7.6)
[Ni(L)(MePhCHNH$_2$)]	11	17.5	12	10.5	(24.4 25.7)
[Ni(HL)(MePhCHNH$_2$)]$^+$	data not available			30.3	(39.0 10.2)

these similarities, the NLO properties will be reported and carefully analyzed for H_2L and [Ni(L)(MePhCHNH$_2$)] only.

NLO Properties. The NLO data are reported in Table 4. Besides a tendency for reduced ZINDO-calculated values compared to the EFISH data, it appears clearly that the nickel complex exhibits a lower NLO response (than that of its related ligand) at both experimental and theoretical levels. This effect strongly contrasts with the previous report of β enhancement by nickel complexation that was obtained in the symmetric and related bis(salicylaldiminato) nickel complex containing the same nitrile withdrawing units.[34] It also contrasts with the general observation by Di Bella et al. that metal complexation in salen and salophen symmetric ligands leads to β enhancement through an additional metal-to-ligand charge transfer.[15] The ZINDO analysis is applied to investigate the microscopic origin of this unexpected behavior.

Within the framework of sum-over-state (SOS) perturbation theory, β is related to all excited states of the molecule[28] and can be expressed as the sum of two contributions, the so-called "two-level" (β_{2L}) and "three-level" (β_{3L}) terms. As observed in most NLO chromophores, β is dominated by β_{2L} in H_2L (Table 4), which allows us to relate the NLO response to the optical transitions according to the following relation:[30a,39]

$$\beta_{2L} = \sum_i \frac{3e^2\hbar f_i \Delta\mu_i}{2mE_i^3} \times \frac{E_i^4}{(E_i^2 - (2\hbar\omega)^2)(E_i^2 - (\hbar\omega)^2)} \quad (3)$$

In this equation, f_i, $\Delta\mu_i$, and E_i are the oscillator strength, the difference between ground and excited-state dipole moments, and the energy of the ith transition, respectively, ($\hbar\omega$ being the energy of the incident laser beam). The calculation reveals that a single low-lying $1 \rightarrow 2$ transition contributes 54% to the total β_{2L}. It is therefore assumed that understanding this transition can account for a qualitative understanding of the NLO response. Ninety-three percent of the transition is described as the HOMO $\rightarrow$ LUMO excitation (Table 3). These orbitals are shown in Figure 5. A charge transfer is clearly evidenced, with 43.7% of the electron density located on the dimethylaminophenyl moieties at the HOMO level and 48.9% of the electron density located on the maleonitrile counterpart at the LUMO level. This accounts for the optical nonlinearity of the ligand unambiguously.

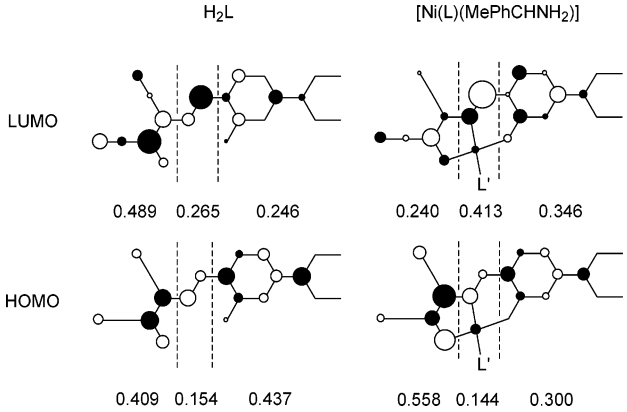

Figure 5. Frontier orbitals with electron densities involved in the low-lying charge-transfer transition responsible for the molecular NLO response of H_2L and [Ni(L)(MePhCHNH$_2$)].

In contrast, the NLO response of [Ni(L)(MePhCHNH$_2$)] appears to be slightly dominated by the β_{3L} term (Table 4). β_{3L} encompasses summations of contributions in which the ground state (g) and two excited states (n and n') are involved in terms of the products of transition dipole moments $r_{gn'}r_{n'n}r_{gn}$ (with $r_{12} = \langle\psi_1|r|\psi_2\rangle$).[28,40] Because direct information is not currently available on excited state to excited state ($n \rightarrow n'$) transitions, β analysis is not possible in that case. In most NLO chromophores, β_{3L} scales to roughly 30−50%

(39) Oudar, J. L.; Chemla, J. *J. Chem. Phys.* **1977**, *66*, 2664.
(40) Teng, C. C.; Garito, A. F. *Phys. Rev. Lett.* **1983**, *50*, 350.

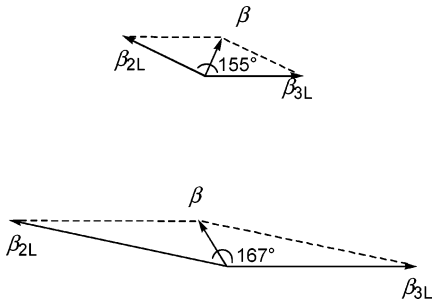

Figure 6. β vector and its β_{2L} and β_{3L} components calculated for [Ni(L)(MePhCHNH$_2$)] at various wavelengths. At 1.907 μm (top), β is directed mostly in the direction of β_{3L} (main β component at low frequency). At 1.064 μm (bottom), β is directed mostly in the direction of β_{2L} (main β component at high frequency), which leads to a β rotation of 45°.

as much as β_{2L} contributions and is of opposite sign (angle of 180°). The reasons for having an NLO response dominated by β_{3L} have not been investigated thoroughly, even if it has been discussed occasionally.[41] However, the deprotonation of the primary amine of H_2L leads to the introduction of a formal but highly donating $-NH^-$ fragment. This is evidenced by the examination of the frontier orbitals in Figure 4. In contrast, versus H_2L, the amido-maleonitrile fragment is turned from an acceptor to an efficient donor in the metal complex, a modification that affects both β_{2L} and β_{3L} necessarily and therefore the overall β. Nevertheless, and because of the complexity of the β_{3L} expression, any attempt to relate β to a set of specific transitions would probably be somewhat irrelevant.

Another unexpected result arises from a careful examination of the ZINDO calculation. If β_{3L} is dominant at lower laser frequency, then the calculation reveals that β_{2L} becomes increasingly important as the frequency increases. Moreover, the angle between β_{2L} and β_{3L} is equal to 155° (instead of 180°). Consequently, the relative increase of β_{2L} leads to a rotation of the overall hyperpolarization ($\beta_{2L} + \beta_{3L}$). This behavior is illustrated in Figure 6. Increasing β values is a well-known trend at higher frequency. However, this tendency usually leaves the β direction unaffected. For instance, the calculation carried out on H_2L indicates a β rotation of 4° as the laser operating wavelength switches from 1.907 to 1.064 μm. In contrast, β undergoes a rotation of about 45° in [Ni(L)(MePhCHNH$_2$)] between 1.907 and 1.064 μm, an effect that arises from the balance between β_{2L} and β_{3L} (Figure 6).

The ultimate understanding of the origin of the β rotation in the nickel complex is hampered by the complexity of β_{3L} (see above). It would imply an understanding of (1) the reason for having an angle of 155 instead of 180° between β_{2L} and β_{3L} and (2) the reason for having β_{2L} increasing more rapidly than β_{3L} at higher frequency. Concerning the first issue, strictly 1D structures possess a unique charge-transfer axis; therefore, the angle between vectors β_{2L} and β_{3L} is equal to 180°. In the present nickel complex, because of reduced 1D character β_{2L} and β_{3L}, which result from the contribution of many *i* transitions, have orientations that are difficult to predict precisely. Even if the angle seems hardly predictable, there is no reason to assume that both vectors are strictly opposite (angle < 180°). As far as the relative β_{2L}/β_{3L} value is concerned, it is obvious that larger β_{2L} values at higher frequencies are related to a resonance effect, according to the last term in eq 3. To the best of our knowledge, the issue of how the magnitude of this effect is transposed into β_{3L} has not been investigated thoroughly, probably because of the high complexity of the β_{3L} expression.[28] This would probably remain a challenge for theorists.

Additionally, [Ni(L)(MePhCHNH$_2$)] crystallizes in the noncentrosymmetric $P2_12_12_1$ space group, which leads to a nonvanishing NLO response in the solid state. The compound therefore exhibits an SHG efficiency roughly equal to 1.25 times that of urea.

Critical Evaluation of NLO Switches Obtained with [Ni(L)(MePhCHNH$_2$)]. Except in the intriguing case of octupolar geometries (e.g., T_d, D_{3h}, D_{2d}),[42] the third-rank β tensor in eq 1 can be restricted to its vectorial component in most molecules. Therefore, the parameter of interest to account for the NLO response is $|\beta| \times |E|^2 \times (\cos\theta)^2$, with θ being the angle between the β vector and E (electric field component of the incident light). The issue of a possible NLO switch by β rotation is therefore naturally addressed, on the basis of the idea that the second-harmonic signal, which is optimized with $\theta = 0°$ (on state), may vanish with $\theta = 90°$ (off state). The ZINDO analysis suggests that the β orientation is strongly dependent on the laser wavelength in the complex and might therefore become perpendicular to that of the ligand at a suitable wavelength. Of course, the design of such a device and its practical use would raise many critical issues, the first one being how to tune reversibly the metal complexation at the molecular level. Certainly, achieving molecular motion has become an important issue in contemporary research.[43] Nature has provided many examples of such devices, each of them occurring in different types of cells for a particular function.[44] However, even if there is no reason to think that molecular engineering will never be able to reach this goal, it seems to be hardly accessible for the present generation of scientists.

A more realistic strategy for a switch induced by β rotation in molecules such as [Ni(L)(MePhCHNH$_2$)] should imply a chemical modification that is easier to monitor than a metal complexation, for instance, a simple protonation. A literature survey conducted on the Cambridge crystallographic database (CCDB) revealed that 41 structures contain the $-NH-Ni^{(II)}$ unit versus 766 based on $-NH_2-Ni^{(II)}$. Among the 41 structures, only 20 are built up from a primary amine, but their synthesis requires the use of a strong base.[45] Therefore, the possible protonation of the actual nickel complex could be envisioned according to the following equation:

$$[Ni(L)(MePhCHNH_2)] + H^+ \rightleftharpoons [Ni(HL)(MePhCHNH_2)]^+ \quad (4)$$

The corresponding proton affinity (PA) is compared to those

(41) See, for example, (a) Lepetit, C.; Lacroix, P. G.; Peyrou, V.; Saccavini, C.; Chauvin, R. J. *Comput. Methods Sci. Eng.* 2004, in press. (b) Di Bella, S.; Fragalà, I. *Eur. J. Inorg. Chem.* **2003**, 2606. (c) Di Bella, S.; Fragalà, I. *New J. Chem.* **2002**, *26*, 285. (d) Kanis, D. R.; Lacroix, P. G.; Ratner, M. A.; Marks, T. J. *J. Am. Chem. Soc.* **1994**, *116*, 10089.

Scheme 3

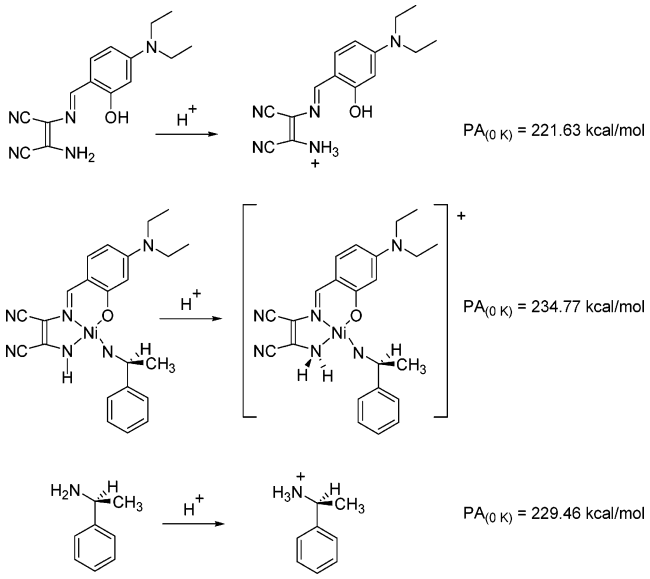

of related amines in Scheme 3 to provide computational support for significant basicity in the $-NH-Ni^{II}$ unit. In particular, the protonation at $-NH-Ni^{II}$ appears to be more favorable than that achieved on the primary $MePhCHNH_2$ amine.

Until now, the intermolecular proton transfer−NLO properties relationship has received very little attention.[46−48] Computationally, $[Ni(HL)(MePhCHNH_2)]^+$ is found to be roughly similar to the parent $[Ni(L)(MePhCHNH_2)]$ chromophore, the most noticeable modification being the elongation of the N(2)−C(13) bond upon protonation from 1.345 to 1.457 Å, consistent with the vanishing donating effect that was observed previously at N(2). Additionally, the conjugated pathway between N(3) (diethylamino) and N(5) (nitrile) is slightly modified (±0.025 Å) by a shortening of the single bonds and an elongation of the double bonds. These modifications lead to restoration of an important electron delocalization between the diethylamino substituent and the maleonitrile moieties. Therefore, the optical properties of $[Ni(HL)(MePhCHNH_2)]^+$ appear to be reminiscent of those of the parent H_2L ligand with an intense charge-transfer transition located at 392 nm ($f = 1.28$) and a weak shoulder at higher energy. This leads to an enhanced β value equal to 30.3×10^{-30} cm^5 esu^{-1} (Table 4). As observed for H_2L, the ZINDO data indicate that β_{2L} dominates the nonlinearity (Table 4) with an intense HOMO → LUMO based transition

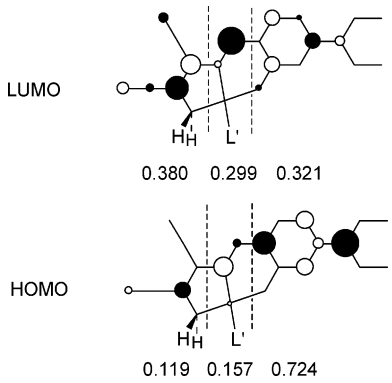

Figure 7. Frontier orbitals with electron densities involved in the low-lying charge-transfer transition responsible for the molecular NLO response of $[Ni(HL)(MePhCHNH_2)]^+$.

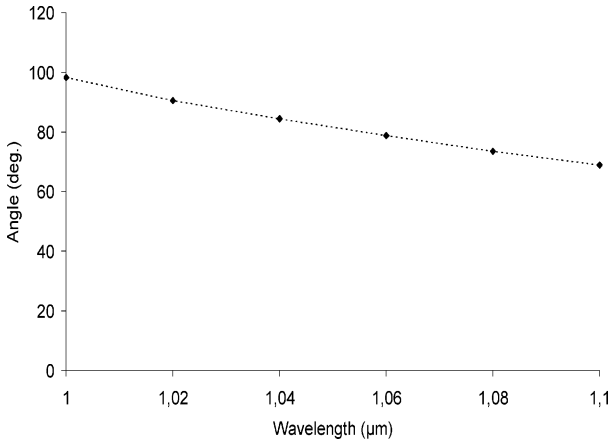

Figure 8. β rotation obtained upon protonation of $[Ni(L)(MePhCHNH_2)]$ into $[Ni(HL)(MePhCHNH_2)]^+$, expressed as a function of the laser wavelength.

being responsible for 44% of the effect. These similarities are illustrated further by the description of the frontier orbitals in Figure 7. As evidenced in H_2L, push−pull character arises from electron density localized mainly on the dimethylaminophenyl at the HOMO level and on the maleonitrile counterpart at the LUMO level. Therefore, β is only weakly subjected to rotation with the laser frequency in H_2L and $[Ni(HL)(MePhCHNH_2)]^+$, in contrast to the situation that is observed in $[Ni(L)(MePhCHNH_2)]$. The β rotation resulting from the protonation of $[Ni(L)(MePhCHNH_2)]$ is illustrated in Figure 8. The angle value is equal to 23.4° at zero frequency ($\lambda \rightarrow \infty$), rises to 29.7° at $\lambda = 1.907$ μm, and then becomes strongly dependent on the laser wavelength. Interestingly, the calculation reveals that the value is strictly equal to 90° at $\lambda = 1.022$ μm, thus providing a potential NLO switch. This intriguing situation, which results from the assumption of a pure vectorial β tensor, has to be discussed with caution. Nevertheless, it suggests that, in this unusual situation, a new type of NLO switch may be envisioned theoretically.

Of course, there would necessarily be many issues to take into account before considering such complexes in a perspective of real application in material chemistry, the first one being the stability of the species in acidic media. It is important to point out that it was not possible to isolate [Ni-

(42) For a general introduction to octupolar molecules, see Zyss, J.; Ledoux, I. *Chem. Rev.* **1994**, *94*, 77.
(43) Molecular Machines, special issue of *Acc. Chem. Res.* **2001**, *34*(6).
(44) Vale, R. D.; Milligan, R. A. *Science* **2000**, *288*, 88.
(45) See, for example, (a) Wilkes, E. N.; Hambley, T. W.; Lawrance, G. A.; Maeder, M. *Aust. J. Chem.* **2000**, *53*, 517. (b) Meyer, F.; Hyla-Kryspin, I.; Kaifer, E.; Kircher, P. *Eur. J. Inorg. Chem.* **2000**, 771. (c) Arion, V.; Wieghardt, K.; Weyhermueller, T.; Bill, E.; Leovac, V. L.; Rufinska, A. *Inorg. Chem.* **1997**, *36*, 661. (d) Richter, R.; Hartung, J.; Beyer, L.; Langer, V. *Z. Anorg. Allg. Chem.* **1993**, *619*, 1295.
(46) Lacroix, P. G.; Lepetit, C.; Daran, J. C. *New J. Chem.* **2001**, *25*, 451.
(47) Evans, C. C.; Bagieu-Beucher, M.; Masse, R.; Nicoud, J.-F. *Chem. Mater.* **1998**, *10*, 847.
(48) Pan, F.; Wong, M. S.; Gramlich, V.; Bosshard, C.; Günther, P. *J. Am. Chem. Soc.* **1996**, *118*, 6315.

$(HL)(MePhCHNH_2)]^+$ by the addition of acid to the solution. Instead, a lowering of the UV−visible band at 486 nm was observed after a few minutes, with the appearance of NMR signals ascribed to H_2L. Therefore, $[Ni(L)(MePhCHNH_2)]$ will certainly not be the ultimate candidate for this type of NLO switch. At a more theoretical level, additional computational approaches could be applied tentatively to verify the ZINDO trends and predictions, for instance, within the newly emerging time-dependent density functional theory (TD-DFT). This method, until now, has shown limited accuracy for describing molecular hyperpolarizabilities of extended π systems.[49,50] Nevertheless, a recent report has pointed out that TD-DFT β values of stilbazolium-type chromophores can agree quite closely with the experimental data.[51] Therefore, this approach will probably be more fruitful in the future. Finally, the experimental issues of how to achieve the proton transfer and how to measure the expected effect cannot be avoided. Protonic conductors are well-known transparent structures that are fully suitable for NLO applications.[52,53] Some of them (e.g., those based on phosphates or phosphonates)[54] could lead to hybrid organic−inorganic networks with potential NLO and proton-transfer behaviors.

(49) For critical reviews on β calculations by TD-DFT, see (a) Money, V. *Khim. Fakultet* **2001**, *91*, 69 and 85. (b) Matsuzawa, N. N.; Dixon, D. A. *Mol. Cryst. Liq. Cryst. Sci. Technol., Sect. B* **2000**, *26*, 17. (c) Monev, V. *Mol. Eng.* **1999**, *8*, 217.

(50) For examples of limitation of the NLO response estimation by means of TD-DFT, see (a) Cai, Z. L.; Sendt, K.; Reimers, J. R. *J. Chem. Phys.* **2002**, *117*, 5543. (b) Van Gisbergen, S. J. A.; Schipper, P. R. T.; Gritensko, O. V.; Baerends, E. J.; Snijders, J. D.; Champagne, B.; Kirtman, B. *Phys. Rev. Lett.* **1999**, *83*, 694. (c) De Boeij, P. L.; Kootstra, F.; Berger, J. A.; Van Leeuwen, R.; Snijders, J. G. *J. Chem. Phys.* **2001**, *115*, 1995.

(51) Coe, B. J.; Harris, J. A.; Brunschwig, B. S.; Garin, J.; Orduna, J.; Coles, S. J.; Hursthouse, M. B. *J. Am. Chem. Soc.* **2004**, *126*, 10418.

(52) (a) Protonic Conductors. Special issue of *Solid State Ionics* **2001**, *145*. (b) Solid State Protonic Conductors. Special issue of *Solid State Ionics* **1997**, *97*.

(53) *Protonic Conductors*; Colomban, Ph., Ed.; Cambridge University Press: Cambridge, U.K. 1992.

(54) For a review on PO_4^{3-}- and $RP(O)(OMe)_2$-based protonic conductors, see, for example, Alberti, G.; Casciola, M. *Chem. Solid State Mater.* **1992**, *2*, 238.

Conclusions

Several new nickel(II) complexes that were obtained from a tridentate (H_2L) Schiff-base ligand have been reported. The synthetic process leads to the formation of the rather unusual nickel−amido ($-NH-Ni^{II}$) bond by deprotonation of the primary amine located on H_2L. The proton affinities estimated by DFT indicate that the ($-NH-Ni^{II}$) group is more basic than a primary amine, although the chemical stability of the resulting $(-NH_2-Ni^{II})^+$-containing species is very poor. ZINDO calculations suggest that the β orientation in $[Ni(L)(MePhCHNH_2)]$ is surprisingly strongly dependent on the laser frequency, which is in strong contrast to that in $[Ni(HL)(MePhCHNH_2)]^+$. A careful examination reveals that the β rotation that is achieved upon protonation of $[Ni(L)(MePhCHNH_2)]$ is precisely equal to 90° when the laser is operating at 1.022 μm.

Until now, switching the NLO response of a molecule has been achieved in only a few instances. The present investigation points out for the first time that a switch obtained by β rotation of 90° could be envisioned within a single molecule. We are now considering the possibility of carrying out frequency-dependent NLO measurements on chiral single crystals to test the real potential of these metal complexes as molecular materials with switching NLO capabilities. The study of the frequency dependence of the EFISH signal could also be envisioned for a better understanding of the NLO response in these molecules.

Acknowledgment. We thank CALMIP (CALcul en Midi Pyrénées − Toulouse) for parallel computing facilities.

Supporting Information Available: Gas-phase structures of H_2L, $[Ni(L)(MePhCHNH_2)]$, and $[NiH(L)(MePhCHNH_2)]^+$. X-ray crystallographic files including the structural data for H_2L, $[Ni(L)(MePhCHNH_2)]$, and $[Ni(L)(^iPrNH_2)]$ in CIF format have been deposited with the Cambridge Crystallographic Data Centre (numbers CCDC 243546, CCDC 243547, and CCDC 243548, respectively). This material is available free of charge via the Internet at http://pubs.acs.org.

IC048578N